RSC Advances

PAPER

View Article Online
View Journal | View Issue

Cite this: *RSC Adv.*, 2022, **12**, 29777

Syntheses and properties of tri- and multi-block copolymers consisting of polybutadiene and polylactide segments

Zhengyue Wang, Yue Zhao and Yuhan Wei *

Received 12th August 2022
Accepted 11th October 2022

DOI: 10.1039/d2ra05051j

rsc.li/rsc-advances

Biomaterials have drawn considerable attention in recent years because of environmental concerns. In this paper, several different poly(lactide)-*b*-poly(butadiene)-*b*-poly(lactide) (PLA-*b*-PB-*b*-PLA) triblock copolymers were synthesized by the bulk ring-opening polymerization of lactide initiated by flexible macro-initiator hydroxyl-terminated polybutadiene (HTPB) by adjusting the ratio of HTPB to lactide and the optical isomer of lactide. Afterwards, a chain-extension reaction with hexamethylene diisocyanate (HDI) was carried out to prepare (PLA-*b*-PB-*b*-PLA)$_n$ multi-block copolymers with enhanced molecular weight. The structures and properties of these block copolymers were then characterized by gel permeation chromatography (GPC), nuclear magnetic resonance (NMR), differential scanning calorimetry (DSC), atomic force microscope (AFM) and Fourier-transform infrared (FTIR). Toughening effect of the (PLA-*b*-PB-*b*-PLA)$_n$ multiblock copolymers on biodegradable poly(L-lactide) (PLLA) film was investigated and the blended film with higher (poly(D-lactide)-*b*-poly(butadiene)-*b*-poly(D-lactide))$_n$ (PDLA-*b*-PB-*b*-PDLA)$_n$ loading (15 wt%) exhibited better toughness nearly without loss of the tensile strength. The mechanical properties of the (PLA-*b*-PB-*b*-PLA)$_n$/PLLA blended film were proved to be influenced by the different isomers of PLA and rubbery PB chains.

1. Introduction

Over the past thirty years, there has been an increasing emphasis on the development of biodegradable plastics made from renewable biobased resources as promising replacements for conventional petroleum and nondegradable ones.[1,2] Poly(lactic acid) (PLA) is a kind of typical biodegradable polyester, which is prepared from renewable plant resources or lactide by chemical synthesis[3,4] and has been widely used in biomedical, packaging materials, pharmaceuticals and other fields for its good biocompatibility,[5] degradability[6,7] and processability.[8–10] However, the brittleness of PLA greatly limits the application range of PLA and many strategies have been explored to toughen PLA,[11] including plasticization, blending with flexible polymers and copolymerization *etc*.[12] Among them, polymer blending with a carefully selected component is an efficient and cost-effective method of improving the toughness of PLA. However, toughening enhancement is always accompanied by a deterioration of the mechanical strength. More and more effects have been devoted to toughen PLA without sacrificing of mechanical strength.

Thermoplastic elastomer (TPE) is a linear segmented copolymer with alternating rigid and flexible segments. TPE can obtain rigidity and hardness from the crystalline domain of the hard segment, while the amorphous soft segment provides flexibility and elastic behavior.[13,14] With excellent toughness and elasticity, TPEs can produce large deformation under weak stress and are ideal materials for toughening PLA.[14] Thermoplastic polyurethane (TPU),[15,16] thermoplastic polyester elastomer (TPEE)[17] and polyolefin[18] have been reported to toughen PLLA effectively. Han *et al.* prepared PLA/TPU blends to enhance the elongation at break of PLLA while the yield strength decreased.[19] Ishihara *et al.* increased the toughness of PLA by incorporating thermoplastic elastomers (TPE).[20] Cramail *et al.* used thermoplastic poly(ester-amide) as modifiers to prepare toughened PLA.[21] Recently, Park *et al.* utilized a TPEE to toughen PLLA using a *in situ* nanofibrillation technique, tough and stiff PLLA nanocomposite generated.[22] However, preparation of the stiffness-toughness balanced PLA material by simply blending PLA with TPE has rarely been reported.

Considering the compatibility between PLLA matrix and toughening agent, a series of poly(lactide)-*b*-poly(butadiene)-*b*-poly(lactide) PLA-*b*-PB-*b*-PLA triblock copolymers consisting of flexible PB blocks and rigid PLA blocks were synthesized by the bulk ring-opening polymerization of lactide with different optical activity in this study. It is well known that PLA's raw material lactide has two chiral carbon atoms, so it is possible to prepare poly(L-lactide) (PLLA), poly(D-lactide) (PDLA) and racemic polylactide poly(D, L-lactide) (PDLLA) from lactide with different optical activity. PDLLA-*b*-PB-*b*-PDLLA and PDLA-*b*-PB-

School of Polymer Science & Engineering, Qingdao University of Science and Technology, Qingdao, 266042, China. E-mail: weiyh@qust.edu.cn; Tel: +86 053284022927

b-PDLA triblock copolymers were prepared. Modern synthetic methods allow access to numerous structures of multiblock copolymers, which have attracted interest because they are expected to have distinct microstructures and exhibit different mechanical behavior compared to conventional polymers with simple architectures. Hexamethylene diisocyanate (HDI) was then used as a chain extender for PLA-*b*-PB-*b*-PLA to produce a thermoplastic multiblock copolymers $(PLA\text{-}b\text{-}PB\text{-}b\text{-}PLA)_n$. These tri- and multi-block copolymers demonstrated distinct properties. $(PLA\text{-}b\text{-}PB\text{-}b\text{-}PLA)_n$ multiblock copolymers were then solution blended with PLLA and the toughening effect of the multiblock copolymer on PLLA film was then investigated. The mechanical properties of the $(PLA\text{-}b\text{-}PB\text{-}b\text{-}PLA)_n$/PLLA blended film were proved to be influenced by the different isomers of PLA and rubbery PB chains. Toughened PLLA films without loss of the tensile strength were obtained in $(PDLA\text{-}b\text{-}PB\text{-}b\text{-}PDLA)_n$/PLLA blended film with higher $(PDLA\text{-}b\text{-}PB\text{-}b\text{-}PDLA)_n$ loading (15 wt%) and the stereocomplexation formation played an important role in this circumstance.

2. Experimental

2.1 Materials

Stannous isooctanoate $Sn(Oct)_2$ and HDI were purchased from Aladdin, hydroxyl-terminated polybutadiene (HTPB) was purchased from Energy Chemical (Mn: ~4200 g mol^{-1}). PLLA (4032D) was purchased from NatureWorks. Toluene was refluxed over sodium metal and benzophenone overnight and distilled under nitrogen atmosphere before use. All glassware used were treated with a solution of dichloromethane and dried at 120 °C for 3 h before use.

D-Lactide and D,L-Lactide were purchased from Aladdin and recrystallized before use: put appropriate amount of lactide monomers into a Shrek bottle filled with nitrogen. Add appropriate amount of anhydrous drying toluene solvent in nitrogen atmosphere, then heat the Shrek bottle in an oil bath at 70 °C until the monomer was completely dissolved in toluene, seal it and place in the refrigerator for 24 hours. After that, the single needle was used to transfer the solvent to obtain the crystalline solid. The above process was repeated three times. In the third operation, the solvent was transferred and the cold hydrazine on the back shelf continued to drain the residual solvent to obtain pure and dry recrystallized monomers.

2.2 Measurements and characterization

2.2.1 Nuclear magnetic resonance (NMR). NMR spectra was recorded on a Bruker AVANCE NEO 400 MHz NMR spectrometer (400 MHz for ^{1}H-NMR) at 298 K. Chemical shifts were reported in δ (ppm) with the residual deuterated solvent peak as reference and all NMR spectra were performed in deuterated chloroform (modified according to use of deuterium solvent).

2.2.2 Gel permeation chromatography (GPC). The molecular weight and molecular weight distribution of the polymer were determined by GPC of Waters company. The gel permeation chromatography is equipped with Waters1525 high pressure high performance liquid chromatography pump, Waters2414 difference detector and Waters717 automatic injector. The temperature of the test column is 30 °C. Tetrahydrofuran was used as mobile phase with the flow rate of 1.0 mL min^{-1}, and the standard sample was polystyrene.

2.2.3 Differential scanning calorimetry (DSC). DSC measurements were performed on a TA instrument DSC 25 under a nitrogen atmosphere with a flow rate of 50 mL min^{-1}. Film samples (about 2–5 mg) enclosed in the aluminum pans were first heated from 20 °C to 250 °C at 10 °C min^{-1} and held for 2 min to erase the heat history. It was then cooled down to −80 °C followed by a reheating to 250 °C at 10 °C min^{-1} to examine the thermal properties of the film samples. And the glass transition temperature was obtained from the second heating curves in DSC.

2.2.4 Atomic force microscope (AFM). AFM studies were conducted using tapping mode AFM (Bruker Multimode 8 AFM/SPM system) in ambient air with Nanoscope software.

2.2.5 Fourier-transform infrared analysis (FTIR). FTIR absorption spectra were recorded using an IFS88-IR spectrometer (Bruker AXS GmbH, Karlsruhe, Germany) in the range 400–4000 cm^{-1}. The spectral resolution was 2 cm^{-1}, and 16 scans were averaged for each specimen.

2.2.6 Scanning electronic microscope (SEM). SEM Images were taken on a FEI Quanta 250 instrument, all samples were coated with a thin layer of gold (2–3 nm) prior to imaging.

2.2.7 Tensile property test. Tensile tests were performed with Instron-5943 Solids Analyzer at a crosshead speed of 5 mm min^{-1} at room temperature. Samples for tensile tests were cut from the blended films with a dimension around 60 mm × 5 mm × 0.1 mm. Tensile tests were performed according to the GB/T13022-1991 standard. The results were the average values of at least four specimens.

2.3 Synthesis of PLA-*b*-PB-*b*-PLA triblock copolymers and $(PLA\text{-}b\text{-}PB\text{-}b\text{-}PLA)_n$ multiblock copolymers

According to the previous report,[12] PLA-*b*-PB-*b*-PLA was synthesized as follow. In the glovebox, a round bottom flask was charged with HTPB and $Sn(Oct)_2$ followed by the addition of D,L-Lactide (or D-Lactide). The mixture was heated at 130 °C for 15 min under nitrogen atmosphere with the stirring speed of 200 rpm. And then, the reaction flask was quickly cooled to room temperature with cold water, 2–3 mL dichloromethane was dropped to dissolve all product. After that, about one drop of the liquid was transferred into a centrifuge tube for nuclear magnetic resonance testing, the remaining solution was transferred to a centrifugal tube containing a large amount of cold methanol to precipitate and centrifuge for 3 times. Finally, the product was dried at 45 °C for 24 hours in an oven and white solid powder was obtained.

A typical chain extension was performed as follow. A right amount of PLA-*b*-PB-*b*-PDLA (200 mg) was put into a nitrogen-filled Shrek bottle, then the Shrek bottle was put into the glove box. In the glove box, toluene (5 mL) and $Sn(Oct)_2$ (10 mg) were added into the Shrek bottle. Then, the reaction flask was sealed and removed from the glovebox, HDI (2 mg) was then added and the reaction flask was stirred continued for 7 h at 75

Table 1 Molecular characteristics of PLA-*b*-PB-*b*-PLA and (PLA-*b*-PB-*b*-PLA$_m$)$_n$

Copolymers	Feed ratio[a]	M_n[b] (kDa)	M_n[c] (kDa)	PDI[b]
PDLLA-*b*-PB-*b*-PDLLA$_1$	1 : 200	12.3	25.4	1.41
PDLA-*b*-PB-*b*-PDLA$_1$	1 : 50	6.7	9.3	1.45
PDLA-*b*-PB-*b*-PDLA$_2$	1 : 20	3.2	5.9	1.62
(PDLLA-*b*-PB-*b*-PDLLA$_1$)$_n$	—	36.7	—	1.65
(PDLA-*b*-PB-*b*-PDLA$_1$)$_n$	—	11.5	—	1.87
(PDLA-*b*-PB-*b*-PDLA$_2$)$_n$	—	7.8	—	1.73

[a] Feed molar ratio of HTPB/D-lactide. [b] Determined from GPC. [c] Calculated from ^{1}HNMR.

°C. The product was washed with methyl alcohol repeatedly and dried under vacuum at 60 °C for 24 h.

Detailed information of the copolymers was listed in Table 1.

2.4 Preparation of (PLA-*b*-PB-*b*-PLA)$_n$/PLLA blend film samples

The blends of multiblock copolymer and PLLA (4032D) were fabricated as following. (PLA-*b*-PB-*b*-PLA)$_n$ multiblock copolymers and PLLA were dissolved in dichloromethane and stirred for more than 48 hours at room temperature. The solution concentration was 50 mg mL^{-1}. The sample films were prepared by solvent casting from (PLA-*b*-PB-*b*-PLA)$_n$/PLLA mixed solution in dichloromethane at room temperature.

3. Results and discussion

3.1 Synthesis of PLA-*b*-PB-*b*-PLA$_m$ triblock copolymers and (PLA-*b*-PB-*b*-PLA$_m$)$_n$ multiblock copolymers

Firstly, HTPB was used as the macromolecular initiator to initiate the ring-opening polymerization of lactide. Take the D,L-lactide as an example, synthesis of the PDLLA-*b*-PB-*b*-PDLLA triblock copolymer was shown in Scheme 1.

Fig. 1 showed a typical ^{1}H-NMR spectrum of the block copolymer PDLLA-*b*-PB-*b*-PDLLA. ^{1}H-NMR spectra of the PDLLA-*b*-PB-*b*-PDLLA block copolymers and HTPB had the characteristic signals of the related polymer blocks. The conversion of the polymer could also be calculated from the ratio of the integral area of H.

According to the attribution of each peak in the Fig. 1, it could be further confirmed that lactide has been connected to HTPB, and the PDLLA-*b*-PB-*b*-PDLLA block copolymer was

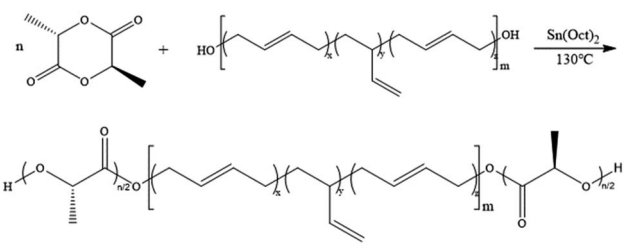

Scheme 1 Synthesis of the PDLLA-*b*-PB-*b*-PDLLA triblock copolymer.

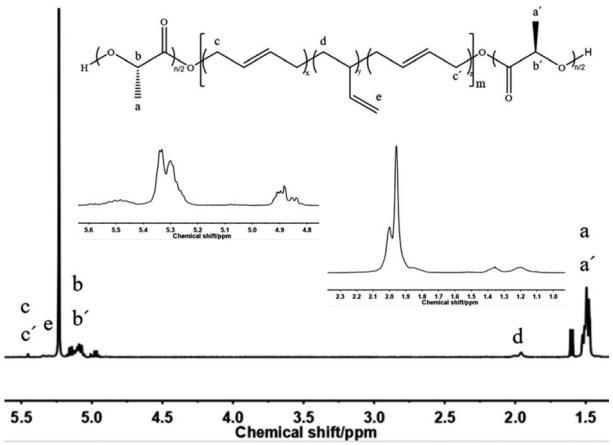

Fig. 1 ^{1}H-NMR spectrum of PDLLA-*b*-PB-*b*-PDLLA, δ 1.45–1.48 (–CH$_3$ of PDLLA), 5.10–5.20 (–O–CH– of PDLLA), 1.56–1.60 (–CH$_3$ of D,L-LA), 4.95–5.00 (–O–CH– of D,L-LA), 1.85–2.15 (–CH$_2$– of 1,2-PB), 4.98–4.94 (=CH$_2$ of 1,2-PB), 5.25–5.39 (=CH– of 1,4-PB).

obtained. The ^{1}H-NMR spectrum of PDLA-*b*-PB-*b*-PDLA was similar and not described here. GPC traces of these PLA-*b*-PB-*b*-PLA were demonstrated in Fig. 2.

And then, the (PLA-*b*-PB-*b*-PLA)$_n$ multiblock copolymers were prepared by chain extension of the PLA-*b*-PB-*b*-PLA$_m$ triblock copolymers with HDI. The FTIR spectra of the PDLA-*b*-PB-*b*-PDLA$_m$ triblock copolymer and (PDLA-*b*-PB-*b*-PDLA$_m$)$_n$ multiblock copolymer were shown in Fig. 3. All of the characteristic absorption peaks of PDLA blocks could be observed in the spectra.[23–25] In particular, the peak at 1530 cm^{-1}(attributed to amino bending) indicated that the isocyanate group had changed into carbamate.[26] In addition, a peak attributed to amino stretching appeared in the region at approximately 3350 cm^{-1} when isocyanate groups were bonded, and the spectrum for the HDI blend specimen clearly showed peaks attributed to the HDI isocyanate group (the peak at

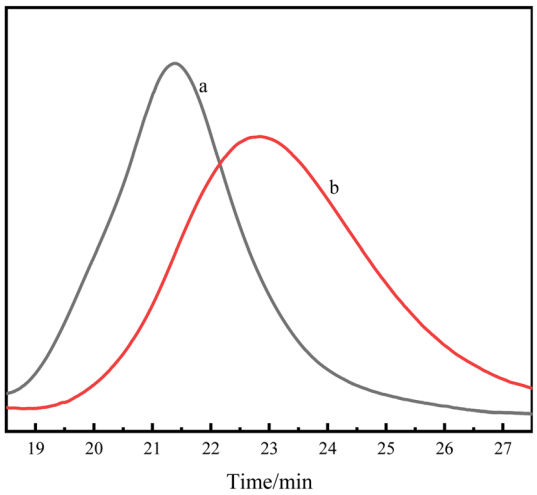

Fig. 2 GPC traces of (a) PDLLA-*b*-PB-*b*-PDLLA$_1$, (b) PDLA-*b*-PB-*b*-PDLA$_2$.

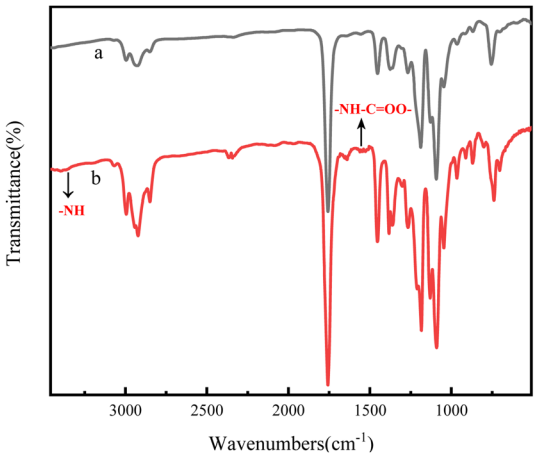

Fig. 3 FTIR spectra of the block copolymer (a) PDLA-*b*-PB-*b*-PDLA$_m$ (b) chain extended (PDLA-*b*-PB-*b*-PDLA)$_n$.

approximately 2340 cm^{-1} correspond to the isocyanate group of HDI), suggesting that multiblock copolymer (PDLA-*b*-PB-*b*-PDLA)$_n$ has been successfully prepared.

Several PLA-*b*-PB-*b*-PLA$_m$ triblock copolymers were successfully synthesized by changing the feed ratio of initiator HTPB to lactide or the optical isomer of the lactide, and the respective (PLA-*b*-PB-*b*-PLA$_m$)$_n$ multiblock copolymers were also prepared. The molecular weight and polydispersity (PDI) of these copolymers were summarized in Table 1.

3.2 Thermal properties of PLA-*b*-PB-*b*-PLA and (PLA-*b*-PB-*b*-PLA)$_n$ copolymers

Fig. 4 showed the first and second heating curves of block copolymers studied in this research. Obvious melting peaks were observed in the first heating curves of PDLA-*b*-PB-*b*-PDLA$_m$ and (PDLA-*b*-PB-*b*-PDLA$_m$)$_n$ since PDLA was crystallizable, while no melting peak was observed in the heating curves of PDLLA-*b*-PB-*b*-PDLLA$_1$ and (PDLLA-*b*-PB-*b*-PDLLA$_1$)$_n$ since PDLLA was amorphous. The first heating curves in Fig. 4(1) showed clearly the crystalline peaks at around 80 °C and the respectively melting peaks at about 160 °C. The melting peaks all disappeared at the second heating curves which were shown in Fig. 4(2). It was deduced that some crystalline aggregates might formed in the procedure of sample preparation for the solvent evaporation, which subsequently induced the cold-crystallization in the first heating process in DSC test. After eliminating the thermal history, considering that polylactic acid was a semi-crystalline material with a low crystallization rate, the temperature rising and cooling rate might be too fast in the DSC test to make a full and complete crystallization, thus no obvious melting peak could be observed in the secondary heating process.

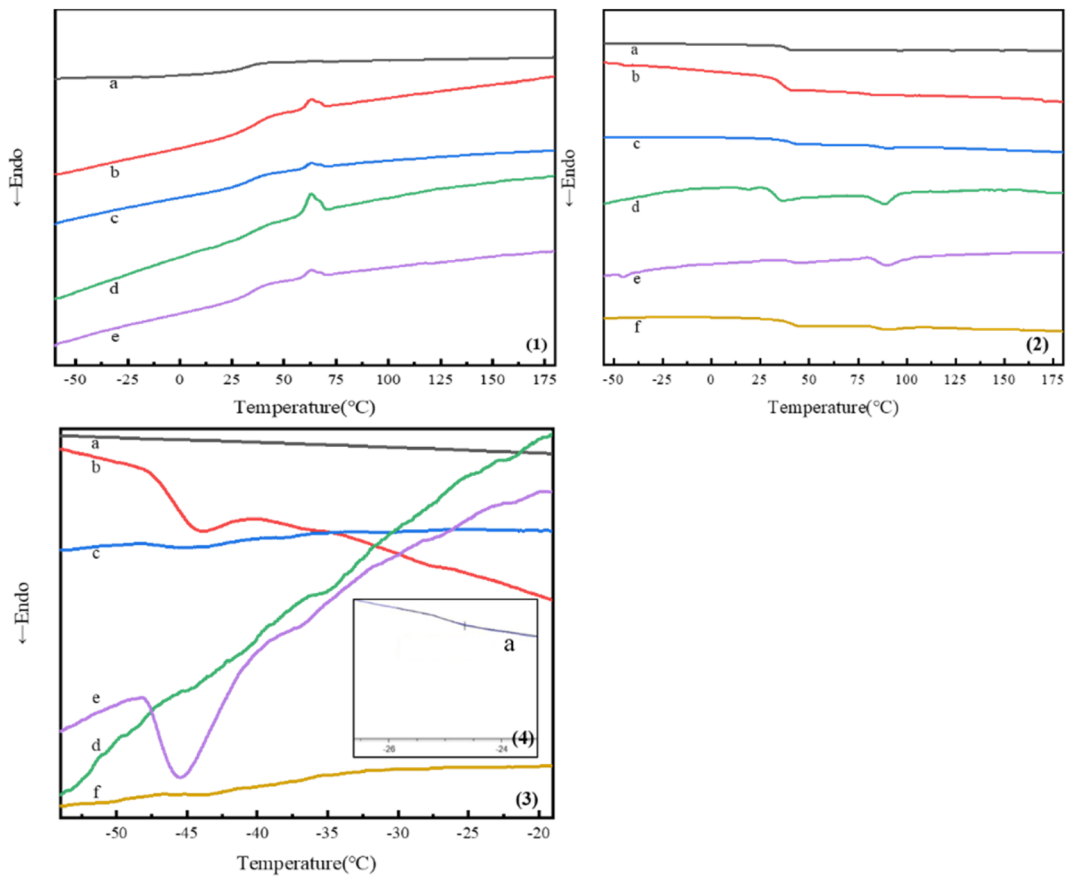

Fig. 4 DSC first heating curves (1) and second heating curves (2) of copolymer films (a) PDLLA-*b*-PB-*b*-PDLLA$_1$ (b) PDLA-*b*-PB-*b*-PDLA$_1$ (c) PDLA-*b*-PB-*b*-PDLA$_2$ (d) (PDLLA-*b*-PB-*b*-PDLLA$_1$)$_n$ (e) (PDLA-*b*-PB-*b*-PDLA$_1$)$_n$ (f) (PDLA-*b*-PB-*b*-PDLA$_2$)$_n$, (3 and 4) is the magnified curves of (2).

Table 2 Thermal properties of triblock copolymers and multiblock copolymer

Copolymers	$T_{g,PB}$ (°C)	$T_{g,PLA}$ (°C)	$T_{c,c}$ (°C)	$\triangle H_{c,c}$ (J g^{-1})	$T_m{}^1$ (°C)	$\triangle H_m{}^1$ (J g^{-1})
PDLLA-*b*-PB-*b*-PDLLA$_1$	−24.95	39.58	—	—	—	—
PDLA-*b*-PB-*b*-PDLA$_1$	−43.23	38.28	64.05	3.84	163.12	34.28
PDLA-*b*-PB-*b*-PDLA$_2$	−45.07	39.63	75.28	12.08	162.48	33.47
(PDLLA-*b*-PB-*b*-PDLLA$_1$)$_n$	−35.09	49.89	—	—	—	—
(PDLA-b-PB-*b*-PDLA$_1$)$_n$	−45.83	40.37	85.46	17.96	156.29	41.19
(PDLA-b-PB-*b*-PDLA$_2$)$_n$	−47.48	40.39	103.00	22.62	160.93	53.30

As shown in the second heating curves of the copolymers in Fig. 4(2 and 3), all triblock and multiblock copolymer samples showed two different glass transition temperature (T_g), which indicated microphase separation in the condensed PB and PLA phases. The T_g for the PB block was captured in the range of −20 °C to −50 °C for all the copolymers, whereas the T_g for the PLA block was recorded in the range of 35 °C to 50 °C. It is well known that T_g of PB homopolymer is about −60 °C, and that of PLA homopolymer is about 60 °C. After magnifying part of the heating curve, obvious glass transition temperature of PB blocks was observed at around −40 °C(shown in Fig. 4(3)). While in Fig. 4(2), an obvious T_g for PLA was observed at around 40 °C, T_g of PB chains increases and T_g of PLA chains decreases in these copolymers. For the synthesized block copolymers, the two block chains have their own glass transition temperature and the characteristic temperature of the block copolymers varies according to the compatibility and phase separation degree of the two block chains. When the compatibility of the two block parts was poor, phase separation occurred and two independent glass transition temperatures consistent with that of homopolymer were observed. However, with the improvement of compatibility, the two characteristic temperatures were gradually close to each other, and finally only one glass transition temperature were observed when completely compatible. In this study, it can be deduced that the compatibility of the PLA and PB was partially miscible. In addition, with increasing of the PB weight fraction and decreasing of the PLA weight fraction in triblock copolymers, T_g of PB chains always decreased and that of PLA chains increased as demonstrated in Table 2. For the multiblock copolymer of (PDLA-*b*-PB-*b*-PDLA$_2$)$_n$, T_g of PB decreased and T_g of PDLA increased as compared with that of PDLA-*b*-PB-*b*-PDLA$_2$ triblock copolymer for the increase of the molecular weight caused by chain extension. Specific data were shown in Table 2.

3.3 Microstructure of the PLA-*b*-PB-*b*-PLA and (PLA-*b*-PB-*b*-PLA)$_n$ copolymer films

Microstructure of the triblock copolymers and multiblock copolymers synthesized by lactide with different optical activity were investigated here. Fig. 5 displayed the morphologies of these copolymer films spin-coated from dichloromethane, in which dichloromethane was a neutral solvent for PB and PLA

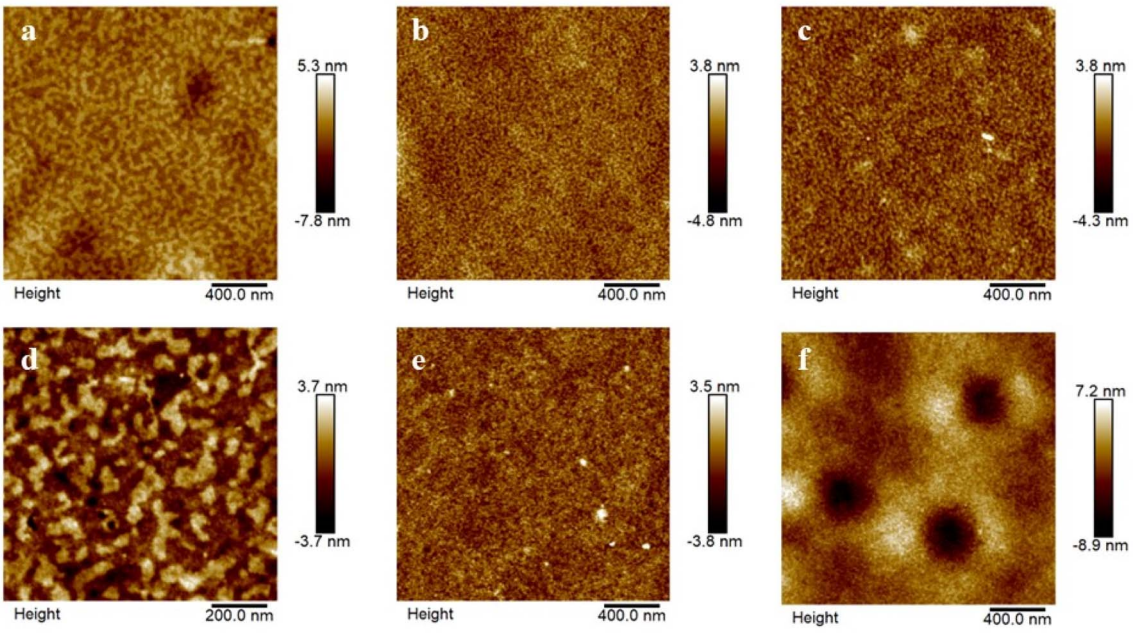

Fig. 5 AFM images of (a) PDLLA-*b*-PB-*b*-PDLLA$_1$ (b) PDLA-*b*-PB-*b*-PDLA$_1$ (c) PDLA-*b*-PB-*b*-PDLA$_2$ (d) (PDLLA-*b*-PB-*b*-PDLLA$_1$)$_n$ (e) (PDLA-*b*-PB-*b*-PDLA$_1$)$_n$ (f) (PDLA-*b*-PB-*b*-PDLA$_2$)$_n$.

blocks, and distinctive microstructures were observed. Legible spinodal microstructure appeared in PDLLA-*b*-PB-*b*-PDLLA thin films for the microphase separation between PB and PDLLA (Fig. 5a). And wormlike phase separated structure was observed in the films of PDLA-*b*-PB-*b*-$PDLA_1$ and PDLA-*b*-PB-*b*-$PDLA_2$. For the higher molecular weight of the PDLLA-*b*-PB-*b*-PDLLA copolymer, phase separated strength was larger than that of PDLA-*b*-PB-*b*-PDLA as obtained from the microdomain size in respective AFM images. As shown in Fig. 5d–f, the phase separated structure had no great change except the domain size in the following multiblock copolymers films.

3.4 Toughen effect of the multiblock copolymers on PLLA

Since TPE has been widely used to toughen polymers, the toughen effect of the multiblock copolymer (PDLLA-*b*-PB-*b*-PDLLA)$_n$ and (PDLA-*b*-PB-*b*-PDLA)$_n$ with higher PB fraction on PLLA was investigated here. Stress–strain measurements were performed on (PDLLA-*b*-PB-*b*-PDLLA)$_n$/PLLA and (PDLA-*b*-PB-*b*-PDLA)$_n$/PLLA blend films to determine the effect of (PDLLA-*b*-PB-*b*-PDLLA)$_n$ and (PDLA-*b*-PB-*b*-PDLA)$_n$ on the mechanical strength of PLLA, which were shown in Fig. 6. As shown in Table 3, the neat PLLA showed its brittle nature with high tensile strength (~62.68 MPa) and low elongation at break (~2.39%). For blends of (PDLA-*b*-PB-*b*-$PDLA_2$)$_n$/PLLA, the amazing result was obtained from elongation at break, which increased to 40% when 5 wt% (PDLA-*b*-PB-*b*-$PDLA_2$)$_n$ was added while decreased to 15% when 15 wt% (PDLA-*b*-PB-*b*-$PDLA_2$)$_n$ was added.[27] And the tensile strength of (PDLA-*b*-PB-*b*-$PDLA_2$)$_n$/PLLA (15 wt : 85 wt) was a bit higher than that of pure PLLA, while the tensile strength of (PDLA-*b*-PB-*b*-$PDLA_2$)$_n$/PLLA (5 wt : 95 wt) decreased a lot. This phenomena might be caused by the existence of physical cross-linking structure formed by stereocomplexation between PDLA-*b*-PB-*b*-PDLA and PLLA matrix which would be discussed below. For blends of (PDLLA-*b*-PB-*b*-PDLLA)$_n$/PLLA, the amazing results was obtained from elongation at break, which increased to 36% when 10 wt% (PDLLA-*b*-PB-*b*-PDLLA)$_n$ was added and decreased to 25% when 5 wt% (PDLLA-*b*-PB-*b*-PDLLA)$_n$ was added. For the (PDLLA-*b*-PB-*b*-PDLLA)$_n$/PLLA blended film, the tensile strength was much lower than that of neat PLA, which may be due to the fact that PDLLA was an amorphous polymer and a stereo crystal coupled not form. The PB particles dispersed in the PLLA matrix acted as toughening part, leading to the increase of ductility of the blends.

Meanwhile, tensile-fractured surface morphologies of the (PDLA-*b*-PB-*b*-PDLA)$_n$/PLLA (15 wt : 85 wt) blend film was then characterized by SEM. The neat PLLA displayed a smooth surface (Fig. 7(1)) implying a brittle fracture. Compared with the surface of the neat PLLA, surface of the (PDLA-*b*-PB-*b*-$PDLA_2$)$_n$/PLLA(15 wt : 85 wt) blend film became very rough. Obvious shear yield of PLLA matrix with some fibrils was observed which would dissipate the energy effectively, leading to an improved strain of PLLA blend film at room temperature.

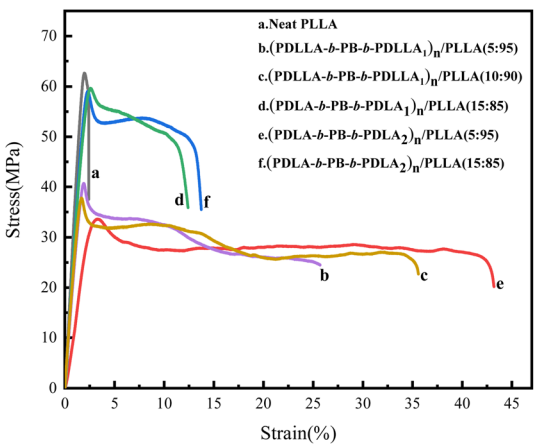

Fig. 6 Stress–strain curves of the PLA-*b*-PB-*b*-PLA/PLLA blended films.

Table 3 Mechanical properties of the multiblock copolymers toughened PLLA

Copolymers	Stress (MPa)	Strain (%)
Neat PLLA	62.68	2.39
(PDLLA-*b*-PB-*b*-$PDLLA_1$)$_n$/PLLA(5 wt : 95 wt)	40.73	25.69
(PDLLA-*b*-PB-*b*-$PDLLA_1$)$_n$/PLLA(10 wt : 90 wt)	37.81	35.56
(PDLA-*b*-PB-*b*-$PDLA_1$)$_n$/PLLA(15 wt : 85 wt)	59.73	12.38
(PDLA-*b*-PB-*b*-$PDLA_2$)$_n$/PLLA(5 wt : 95 wt)	33.63	43.17
(PDLA-*b*-PB-*b*-$PDLA_2$)$_n$/PLLA(15 wt : 85 wt)	58.94	13.74

3.5 Stereocomplexation formation in (PDLA-*b*-PB-*b*-PDLA)$_n$/PLLA blend film

It is well known that stereocomplexation always form by blending of enantiomeric PLLA and PDLA and PLA stereocomplexation also exhibit increased tensile strength and modulus comparing with the homopolymers.[28,29] The melting peaks at about 210 °C assigned to the stereocomplexation were clearly observed in the first heating curves of (PDLA-*b*-PB-*b*-PDLA)$_n$/PLLA blend films in Fig. 8(1), while there was no stereocomplex crystals formed in the (PDLLA-*b*-PB-*b*-PDLLA)$_n$/PLLA blended film. The melting peaks assigned to the stereocomplex became more apparent with the increase of multiblock copolymer content[30] in (PDLA-*b*-PB-*b*-PDLA)$_n$/PLLA blended films. The stereocomplexation formation was also proved by FTIR spectra in Fig. 8(2), the band at 909 cm^{-1} characteristic of the 3_1 helix associated with the stereocomplex was present.[31] The existence of physical cross linking structure formed by stereocomplexation between PDLA-*b*-PB-*b*-PDLA and PLLA matrix might keep the tensile strength at high level for the blend with higher PDLA content and the toughening effect brought by the PB phase was weak. On the other hand, for the blend of (PDLA-*b*-PB-*b*-$PDLA_2$)$_n$/PLLA with lower (PDLA-*b*-PB-*b*-$PDLA_2$)$_n$ content (5 wt%), the melting peak in DSC curve and the band in FTIR spectra ascribed to the stereocomplexation were very tiny, which implied few stereocomplexation formed in this case. So the presence of the stereocomplexation nearly had no contribution to the tensile strength of the blend film. In this situation, the PB particles dispersed in the PLLA matrix acted as toughening part,

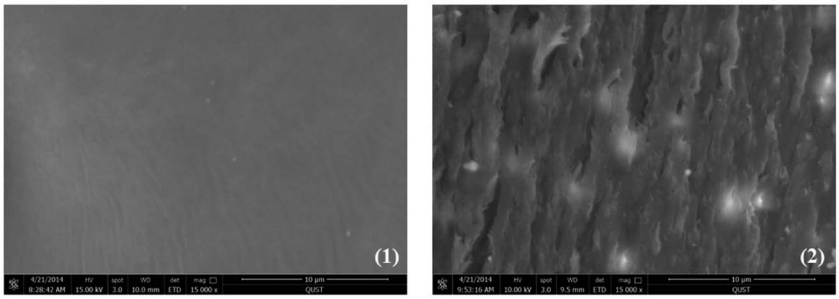

Fig. 7 SEM images of fractured surface morphologies of the tensile films: (1) neat PLLA (2) (PDLA-b-PB-b-PDLA$_2$)$_n$/PLLA(15 wt : 85 wt).

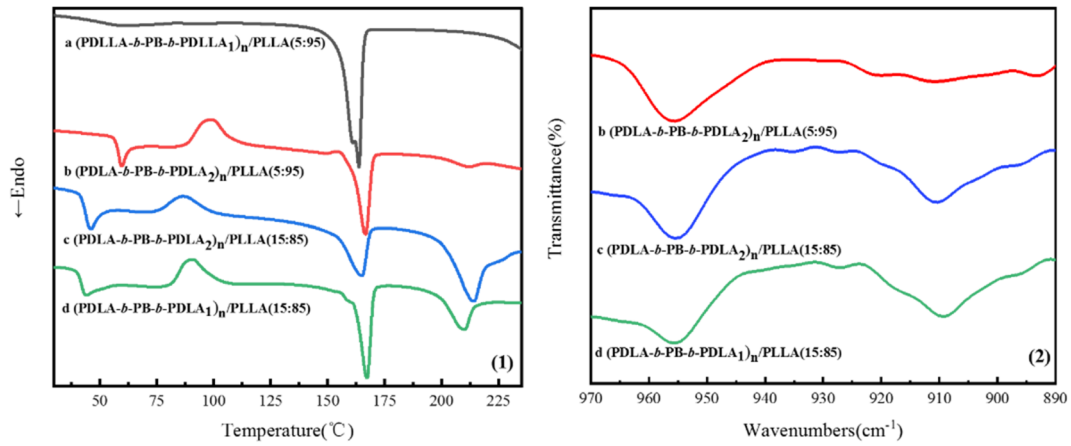

Fig. 8 DSC first heating curves (1) and FTIR spectra (2) of the (PLA-*b*-PB-*b*-PLA)$_n$/PLLA blended films.

leading to the increase of ductility of the blends and the tension strength decreased for the introduction of flexible PB chains.

4. Conclusion

Triblock copolymers PLA-*b*-PB-*b*-PLA synthesized by lactide with different optical activity and respective multiblock copolymer (PLA-*b*-PB-*b*-PLA)$_n$ were synthesized in this study. All block copolymers showed two T_g in their cooling scans indicating phase separation supported by AFM analysis. Toughen effect of the multiblock copolymer (PLA-*b*-PB-*b*-PLA)$_n$ on PLLA was investigated. Addition of (PLA-*b*-PB-*b*-PLA)$_n$ multiblock copolymer toughened the PLLA film to some extent. The (PDLA-*b*-PB-*b*-PDLA)$_n$/PLLA blend film with higher (PDLA-*b*-PB-*b*-PDLA)$_n$ loading (15 wt%) exhibited better toughness nearly without loss of the tensile strength, while the blend film with lower (PDLA-*b*-PB-*b*-PDLA)$_n$ loading (5 wt%) was toughened obviously accompanying with decrease of the tensile strength. The unique mechanical behavior could be explained by the synergistic effect of the stereocomplexation between PDLA-*b*-PB-*b*-PDLA and PLLA, and the rubbery PB chains. While for the toughened (PDLLA-*b*-PB-*b*-PDLLA)$_n$/PLLA blend film, the tensile strength was lower than that of neat PLA, which might be due to the fact that PDLLA was an amorphous polymer and blends could not form a stereo crystal. Therefore, only the PB particles dispersed in the PLLA matrix played a role in toughening, which improved the ductility of the blend without maintaining the tensile strength.

Conflicts of interest

The authors declare no competing financial interest.

Acknowledgements

This work was supported by the National Natural Science Foundation of China (21704052).

References

1 R. A. Sheldon and M. Norton, Green chemistry and the plastic pollution challenge: towards a circular economy, *Green Chem.*, 2020, **22**(19), 6310–6322.
2 D. K. Schneiderman and M. A. Hillmyer, 50th Anniversary Perspective: There Is a Great Future in Sustainable Polymers, *Macromolecules*, 2017, **50**(10), 3733–3749.
3 R. M. Rasal, A. V. Janorkar and D. E. Hirt, Poly(lactic acid) modifications, *Prog. Polym. Sci.*, 2010, **35**(3), 338–356.
4 K. Hamad, M. Kaseem, M. Ayyoob, J. Joo and F. Deri, Polylactic acid blends: The future of green, light and tough, *Prog. Polym. Sci.*, 2018, **85**, 83–127.

5 A. G. Mikos, M. D. Lyman, L. E. Freed and R. Langer, Wetting of poly(l-lactic acid) and poly(DL-lactic-co-glycolic acid) foams for tissue culture, *Biomaterials*, 1994, **15**(1), 55–58.

6 R. T. MacDonald, S. P. McCarthy and R. A. Gross, Enzymatic Degradability of Poly(lactide): Effects of Chain Stereochemistry and Material Crystallinity, *Macromolecules*, 1996, **29**(23), 7356–7361.

7 A. Gross Richard and B. Kalra, Biodegradable Polymers for the Environment, *Science*, 2002, **297**(5582), 803–807.

8 H. Tian, Z. Tang, X. Zhuang, X. Chen and X. Jing, Biodegradable synthetic polymers: Preparation, functionalization and biomedical application, *Prog. Polym. Sci.*, 2012, **37**(2), 237–280.

9 P. Pan and Y. Inoue, Polymorphism and isomorphism in biodegradable polyesters, *Prog. Polym. Sci.*, 2009, **34**(7), 605–640.

10 J.-M. Raquez, Y. Habibi, M. Murariu and P. Dubois, Polylactide (PLA)-based nanocomposites, *Prog. Polym. Sci.*, 2013, **38**(10), 1504–1542.

11 X. Hu, T. Su, P. Li and Z. Wang, Blending modification of PBS/PLA and its enzymatic degradation, *Polym. Bull.*, 2018, **75**(2), 533–546.

12 I. Lee, T. R. Panthani and F. S. Bates, Sustainable Poly(lactide-*b*-butadiene) Multiblock Copolymers with Enhanced Mechanical Properties, *Macromolecules*, 2013, **46**(18), 7387–7398.

13 R. J. Gaymans, Segmented copolymers with monodisperse crystallizable hard segments: Novel semi-crystalline materials, *Prog. Polym. Sci.*, 2011, **36**(6), 713–748.

14 X. Zhao, H. Hu, X. Wang, X. Yu, W. Zhou and S. Peng, Super tough poly(lactic acid) blends: a comprehensive review, *RSC Adv.*, 2020, **10**(22), 13316–13368.

15 W. Lin and J.-P. Qu, Enhancing Impact Toughness of Renewable Poly(lactic acid)/Thermoplastic Polyurethane Blends *via* Constructing Cocontinuous-like Phase Morphology Assisted by Ethylene–Methyl Acrylate–Glycidyl Methacrylate Copolymer, *Ind. Eng. Chem. Res.*, 2019, **58**(25), 10894–10907.

16 M. Sun, S. Huang, M. Yu and K. Han, Toughening Modification of Polylactic Acid by Thermoplastic Silicone Polyurethane Elastomer, *Polymers*, 2021, **13**(12), 1953.

17 H. U. Zaman, J. C. Song, L.-S. Park, I.-K. Kang, S.-Y. Park, G. Kwak, B.-s. Park and K.-B. Yoon, Poly(lactic acid) blends with desired end-use properties by addition of thermoplastic polyester elastomer and MDI, *Polym. Bull.*, 2011, **67**(1), 187–198.

18 E. Forghani, H. Azizi, M. Karabi and I. Ghasemi, Compatibility, morphology and mechanical properties of polylactic acid/polyolefin elastomer foams, *J. Cell. Plast.*, 2016, **54**(2), 235–255.

19 J.-J. Han and H.-X. Huang, Preparation and characterization of biodegradable polylactide/thermoplastic polyurethane elastomer blends, *J. Appl. Polym. Sci.*, 2011, **120**(6), 3217–3223.

20 J. Ishihara, M. Harada, K. Nakano and K. Enomoto, Toughening of polylactic acid by blending with thermoplastic elastomer, *AIP Conf. Proc.*, 2016, **1779**(1), 080002.

21 T. Lebarbé, E. Grau, C. Alfos and H. Cramail, Fatty acid-based thermoplastic poly(ester-amide) as toughening and crystallization improver of poly(l-lactide), *Eur. Polym. J.*, 2015, **65**, 276–285.

22 A. Anstey, A. V. Tuccitto, P. C. Lee and C. B. Park, Generation of Tough, Stiff Polylactide Nanocomposites through the *in Situ* Nanofibrillation of Thermoplastic Elastomer, *ACS Appl. Mater. Interfaces*, 2022, **14**(12), 14422–14434.

23 P. Maity, S. Kasisomayajula, V. Parameswaran, S. Basu and N. Gupta, Improvement in Surface Degradation Properties of Polymer Composites due to Pre-processed Nanometric Alumina Fillers, *IEEE Trans. Dielectr. Electr. Insul.*, 2008, **15**, 63–72.

24 R. J. Awale, F. B. Ali, A. S. Azmi, N. I. M. Puad, H. Anuar and A. Hassan, Enhanced Flexibility of Biodegradable Polylactic Acid/Starch Blends Using Epoxidized Palm Oil as Plasticizer, *Polymers*, 2018, **10**(9), 977.

25 B. W. Chieng, N. A. Ibrahim, W. M. Z. W. Yunus and M. Z. Hussein, Poly(lactic acid)/Poly(ethylene glycol) Polymer Nanocomposites: Effects of Graphene Nanoplatelets, *Polymers*, 2014, **6**(1), 93–104.

26 A. Nandiyanto, R. Oktiani and R. Ragadhita, How to Read and Interpret FTIR Spectroscope of Organic Material, *Indones. J. Sci. Technol.*, 2019, **4**, 97–118.

27 X. Xiao, V. S. Chevali, P. Song, B. Yu, Y. Yang and H. Wang, Enhanced toughness of PLLA/PCL blends using poly(d-lactide)-poly(ε-caprolactone)-poly(D-lactide) as compatibilizer, *Compos. Commun.*, 2020, **21**, 100385.

28 B. H. Tan, J. K. Muiruri, Z. Li and C. He, Recent Progress in Using Stereocomplexation for Enhancement of Thermal and Mechanical Property of Polylactide, *ACS Sustainable Chem. Eng.*, 2016, **4**(10), 5370–5391.

29 J. Chen, C. Rong, T. Lin, Y. Chen, J. Wu, J. You, H. Wang and Y. Li, Stable Co-Continuous PLA/PBAT Blends Compatibilized by Interfacial Stereocomplex Crystallites: Toward Full Biodegradable Polymer Blends with Simultaneously Enhanced Mechanical Properties and Crystallization Rates, *Macromolecules*, 2021, **54**(6), 2852–2861.

30 Y. Liu, J. Shao, J. Sun, X. Bian, Z. Chen, G. Li and X. Chen, Toughening effect of poly(D-lactide)-*b*-poly(butylene succinate)-*b*-poly(D-lactide) copolymers on poly(L-lactic acid) by solution casting method, *Mater. Lett.*, 2015, **155**, 94–96.

31 P. Jia, J. Hu, W. Zhai, Y. Duan, J. Zhang and C. Han, Cell Morphology and Improved Heat Resistance of Microcellular Poly(L-lactide) Foam *via* Introducing Stereocomplex Crystallites of PLA, *Ind. Eng. Chem. Res.*, 2015, **54**(9), 2476–2488.